



ChemComm

**Dinitrogen Activation at Chromium by Photochemically
Induced Cr^{II}-C Bond Homolysis**

Journal:	<i>ChemComm</i>
Manuscript ID	CC-COM-05-2024-002387.R1
Article Type:	Communication

SCHOLARONE™
Manuscripts

Data availability statement:

The data supporting this article have been included as part of the Supplementary Information. Crystallographic data for compounds **1**, **2**, and **3** has been deposited at the CCDC under 2353925 (**1**), 2353926 (**2**), 2353927 (**3**) and can be obtained free of charge via www.ccdc.cam.ac.uk/data_request/cif, or by emailing data_request@ccdc.cam.ac.uk, or by contacting The Cambridge Crystallographic Data Centre, 12 Union Road, Cambridge CB2 1EZ, UK; fax: +44 1223 336033.



Dinitrogen Activation at Chromium by Photochemically Induced Cr^{II}–C Bond Homolysis

Received 00th January 20xx,
Accepted 00th January 20xx

DOI: 10.1039/x0xx00000x

www.rsc.org/

Olivia L. Duletski,^a Duncan Platz,^a Charlie J. Pollock,^a Martín A. Mosquera,^a Navamoney Arulsamy,^b and Michael T. Mock^{a,*}

The synthesis of the organochromium(II) complexes [POCOP^{tBu}]Cr(R) (R = *p*-Tol, Bn) are reported. Exposure of [POCOP^{tBu}]Cr(Bn) to visible light promotes homolytic Cr–C_{Bn} bond cleavage and formed {[POCOP^{tBu}]Cr}₂(η¹:η¹-μ-N₂) via a putative [POCOP^{tBu}]Cr(I) species.

Transition metal dinitrogen complexes are traditionally prepared using chemical reductants, or in some cases, from the loss of H₂ from metal hydride precursors to generate a low-valent metal centre capable of coordinating N₂.¹ The binding mode and subsequently the extent of N₂ activation at one or more transition metals are critical parameters that can define the course of subsequent stoichiometric or catalytic N₂ functionalization steps.² Several of the most efficient molecular N₂ fixation catalysts are based on Mo supported by pincer-type ligands³ in which chemical reduction results in the spontaneous cleavage of the N₂ triple bond via a transient M–N₂–M intermediate to form terminal nitride products.⁴ When a M–N₂–M species has been isolated, photolysis is a successful strategy to facilitate N₂ bond cleavage;⁵ however, photochemistry has rarely been used to prepare M–N₂ complexes.⁶

Despite the numerous examples of Mo–N₂ complexes bearing pincer ligands, only two Cr–N₂ pincer complexes have appeared in the literature. Recent reports from the groups of Nishibayashi, and Schneider and Finger used a neutral PCP or anionic PNP pincer ligands (PCP = 1,3-bis((di-*tert*-butylphosphino)methyl)benzimidazol-2-ylidene; PNP = N(CHCHP^{tBu}Bu₂)₂) to prepare [(PCP)Cr⁰(N₂)]₂(μ-N₂)⁷ and [(PNP)Cr^{II}](μ-N₂)₂,⁸ respectively, by chemical reduction of a (pincer)CrCl precursor.

In our continued efforts examining Cr–N₂ chemistry,⁹ we sought to understand and control N₂ activation and

functionalization with Cr using the anionic POCOP^{tBu} ligand (POCOP^{tBu} = C₆H₃-1,3-[OP(^tBu)₂]₂) to make a direct comparison to the N₂ reactivity of the analogous Mo(POCOP^{tBu}) system. Schrock and co-workers reported chemical reduction of [POCOP^{tBu}]MoI₂ formed {[POCOP^{tBu}]Mo(I)(N)}⁻ from spontaneous cleavage of the N₂ triple bond.¹⁰ [(POCOP^{tBu})Mo^{II}(I)]₂(μ-N₂) was proposed to be an intermediate en route to Mo-nitride formation.

We reasoned a “[POCOP^{tBu}]Cr(N₂)” complex would be accessible by chemical reduction of the halide precursor [POCOP^{tBu}]CrBr, reported by Kirchner and co-workers,¹¹ with an alkali metal reductant such as KC₈ or Na/Hg. The addition of 1.1 equiv KC₈ to a red THF solution of [POCOP^{tBu}]CrBr under N₂ or argon results in isolation of a pentane-soluble purple solid. Unfortunately, no diagnostic ν_{N2} bands were identified by IR or Raman spectroscopies. The UV-vis spectrum shows absorption bands in the visible region of the spectrum at λ_{max} = 378, 392, and 519 nm (See ESI†). While the molecular structure has not been determined, elemental analysis confirmed that nitrogen is not present in the reduction product.

Since chemical reduction was not an effective strategy to generate the targeted Cr–N₂ complex, we assessed the possibility of generating [POCOP^{tBu}]Cr(N₂) by thermally promoted homolytic bond cleavage¹² of organochromium(II) complexes, akin to reactivity reported by Smith, Poli, and co-workers using CpCr^{III}[(Xyl)NCMe)₂CH](R) (Ar = Xyl,; R = Bn, CH₂CMe₃) to generate a Cr(II) product.¹³ Two organochromium(II) complexes were prepared by the reaction of [POCOP^{tBu}]CrBr with the desired R₂Mg reagent at room temperature in Et₂O/dioxane. [POCOP^{tBu}]Cr(R) (R = *p*-Tol (**1**) and R = Bn (**2**)) (*p*-Tol = 4-Me-C₆H₄; Bn = CH₂C₆H₅) were isolated as orange and red solids in 76% and 94% crystalline yield, respectively, Fig 1, panel a. **1** and **2** are each high-spin Cr(II) with a μ_{eff} = 4.5 μB, consistent with a S = 2 ground-state. Crystals suitable for X-ray diffraction (XRD) were grown from a concentrated pentane solution stored at –30 °C. The molecular structures of **1** and **2** have similar metric parameters. Fig 1, panel b

^a Department of Chemistry and Biochemistry, Montana State University, Bozeman, MT 59717, USA. E-mail: michael.mock@montana.edu

^b Department of Chemistry, University of Wyoming, Laramie, WY, 82071, USA.

† Electronic Supplementary Information (ESI) available: Experimental procedures, crystallographic details, additional spectroscopic data, and computational details. CCDC 2353925 (**1**), 2353926 (**2**), 2353927 (**3**). For ESI and crystallographic data in CIF or other electronic format see DOI: 10.1039/x0xx00000x

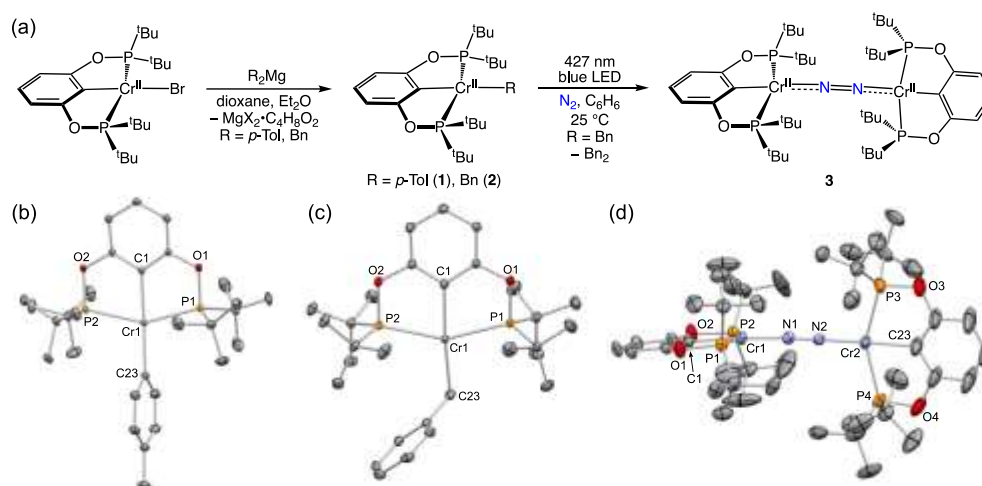


Fig. 1 (a) Synthesis of **1**, **2**, and **3**. Panel (b), (c), and (d) molecular structures of **1**, **2**, and **3**, respectively. Thermal ellipsoids are drawn at 50% probability. Hydrogen atoms are omitted for clarity. Selected bond distances (Å) and angles (°): (**1**) Cr1–C23 = 2.1208(13); Cr1–C1 = 2.1136(12); Cr–P1 = 2.4424(4); Cr–P2 = 2.4487(4); P1–Cr1–P2 = 152.448(14); C1–Cr1–C23 = 174.04(5). (**2**) Cr1–C23 = 2.1735(19); Cr1–C1 = 2.1110(18); Cr–P1 = 2.4557(5); Cr–P2 = 2.4705(5); P1–Cr1–P2 = 152.907(19); C1–Cr1–C23 = 175.10(8). (**3**) Cr1–N1 = 1.843(2); Cr1–C1 = 2.097(3); Cr–P1 = 2.4020(8); Cr–P2 = 2.3807(8); P1–Cr1–P2 = 153.14(3); Cr1–N1–N2 = 176.4(2); Cr2–N2 = 1.836(2); Cr2–C23 = 2.095(3); Cr2–P3 = 2.3722(10); Cr2–P4 = 2.3840(9); P3–Cr2–P4 = 152.69(3); Cr2–N2–N1 = 173.7(2); N1–N2 = 1.192(3).

and c, shows the four-coordinate Cr(II) centre in a pseudo square-planar geometry comprised of two phosphorus atoms, the anionic carbon of the POCOP^tBu backbone, and the C-atom of the *p*-Tol or Bn substituent. The Cr–P and Cr–C(1) bond distances for the POCOP^tBu ligand in **2** are 2.4557(5) Å, 2.4705(5) Å, and 2.1110(18) Å, respectively. The Cr–C(23)_{Bn} bond length in **2** is longer than that of Cr–C(23)_{*p*-Tol} in **1**, at 2.1735(19) Å and 2.1208(13) Å, respectively. Unfortunately, attempts to thermally promote homolytic Cr–C bond rupture to access a reduced Cr complex were unsuccessful. **1** and **2** are stable under N₂ for over two days in refluxing toluene (~110 °C).

Next, we examined visible-light photolysis to promote homolytic Cr–C bond cleavage.¹⁴ Photochemically induced bond cleavage is not uncommon¹⁵; however, the photoinduced loss of an organic moiety and the subsequent binding and activation of N₂ at a metal centre is rare. In the singular example with an azophilic early transition metal, Chirik and co-workers showed the photochemically induced reductive elimination of (*p*-Tol)–(*p*-Tol) from [(η⁵-C₅H₅)₂Zr(*p*-Tol)₂] generated the dinuclear side-on bound dinitrogen complex [(η⁵-C₅Me₄H)₂Zr]₂(μ₂,η²,η²-N₂).^{6a}

Remarkably, photolysis of a benzene solution of **2** with blue light from 427 nm LED lamps under 1 atm N₂ led to a rapid colour change from orange to deep purple, furnishing the dinuclear Cr complex [(POCOP^tBu)Cr]₂(μ-N₂) (**3**) in 73% isolated yield upon recrystallization from pentane, Fig 1, panel a.¹⁶ Formation of bibenzyl (Bn₂) (92% yield by ¹H NMR) indicated Cr–C bond homolysis as a key mechanistic step in the generation of **3** (discussed below). Despite immediate darkening of the solution, photolysis of **2** for ~4–6 h was required for complete conversion to **3**. In benzene or toluene, **3** is stable for extended periods of photolysis, ca. >36 h. Photolysis of **2** in the absence of N₂ generates a

dark red solution along with Bn₂ and toluene formation; however, the Cr product has not been identified. Exposure of the dark red solution to 1 atm N₂ does not form **3**. **1** is unreactive to photolysis with 427 nm light for >24 h, likely a reflection of a stronger Cr–C_{*p*-tolyl} bond.¹⁷

Crystals of **3** for XRD were grown from a concentrated pentane solution stored at –30 °C. The molecular structure in Fig 1, panel d, shows the two (POCOP^tBu)Cr units bridged by an N₂ ligand. The opposing (POCOP^tBu)Cr fragments are rotated 90° with respect to each other to minimize steric interactions of the *tert*-butyl groups. Compared to the precursor **2**, the Cr–P bond lengths in **3** have contracted by ca. ~0.078 Å, with an average Cr–P bond of 2.3847 ± 0.0125 Å. Noting the metrics about the Cr1–N1–N2–Cr2 linkage, the Cr1–N1 and Cr2–N2 bonds are short at 1.843(2) Å and 1.836(2) Å, respectively. The N1–N2 bond distance of 1.192(3) Å indicates significant N₂ activation via Cr back-donation into π* orbitals of N₂, (d_{N–N} free N₂ 1.095 Å), denoting the N₂ ligand, in this case, is best described as an [N₂]²⁻ group bound to two formally Cr(II) centres.

Further support for the assignment of a reduced [N₂]²⁻ ligand was the ν_{NN} band for **3** that was identified in the Raman spectrum at 1639 cm⁻¹ (in pentane). Photolysis of **2** under an atmosphere of ¹⁵N₂ furnished [(POCOP^tBu)Cr]₂(μ-¹⁵N₂) (**3**^{15N}) that displays the expected shift of the ν_{NN} band to 1585 cm⁻¹. Surprisingly, the N₂ ligand in **3** is prone to exchange. Stirring a pentane solution of **3**^{15N} under 1 atm ¹⁴N₂ for 22 h results in ~30% incorporation of ¹⁴N₂ as assessed by Raman data (see ESI†). **3** is stable in THF without the loss of N₂. The structural and spectroscopic features of **3** are comparable to [(PNP)Cr]₂(μ-N₂) reported by Schneider, Finger and co-workers that exhibits an N–N bond length of 1.2080(14) Å, a ν_{NN} = 1651 cm⁻¹ (Raman), and a solution-state magnetic moment of μ_{eff} = 6.3 ± 0.1 μ_B.⁸

Using DFT calculations, $[(\text{PNP})\text{Cr}]_2(\mu\text{-N}_2)$ was best described as two high-spin Cr(II) centres ($S = 2$) antiferromagnetically coupled to the $S = 1$ $[\text{N}_2]^{2-}$ ligand with a $J_{\text{AF}} \approx -1400 \text{ cm}^{-1}$.¹⁸ **3** exhibits a solution-state magnetic moment of $\mu_{\text{eff}} = 6.87 \mu\text{B}$ suggesting a similar electronic structure with a $S_{\text{T}} = 3$ spin-state. However, broken-symmetry DFT calculations of **3** revealed larger antiferromagnetic coupling, $J_{\text{AF}} \approx -3215 \text{ cm}^{-1}$, indicating greater covalency between the Cr(II) centres and $[\text{N}_2]^{2-}$. The UV-Vis spectrum of the deep purple solution of **3** exhibits two intense absorption features at $\lambda_{\text{max}} = 495 \text{ nm}$ ($\epsilon = 9568 \text{ M}^{-1} \text{ cm}^{-1}$) and 578 nm ($\epsilon = 10503 \text{ M}^{-1} \text{ cm}^{-1}$). These diagnostic absorption bands definitively establish that **3** is not generated in the chemical reduction of $[\text{POCOP}^{\text{tBu}}]\text{CrBr}$ with KC_8 (*vide supra*), see ESI†.

A plausible mechanism for the photochemical formation of **3** is depicted in Fig. 2. Photolysis of **2** generates a LMCT excited state resulting in homolysis of the Cr–C_{Bn} bond forming a one-electron reduced (POCOP^{tBu})Cr(I) fragment

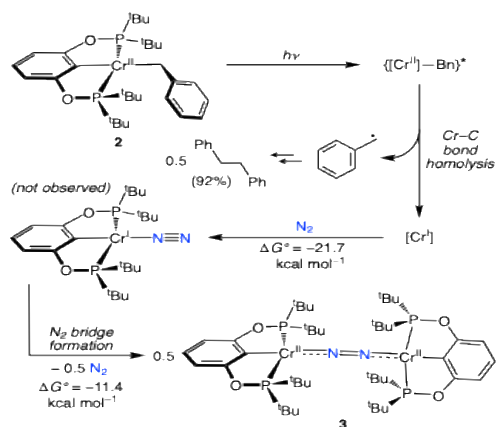


Fig. 2 Proposed mechanism for photochemically induced Cr–C bond homolysis in **2** to form **3**. N_2 coordination to Cr(I) and the generation of **3** upon N_2 bridge formation were assessed by DFT calculations. $[\text{Cr}] = (\text{POCOP}^{\text{tBu}})\text{Cr}$.

and PhCH_2^{\cdot} .¹⁹ Homocoupling of two PhCH_2^{\cdot} leads to bibenzyl formation. The Cr(I) fragment is trapped by N_2 forming a mononuclear $(\text{POCOP}^{\text{tBu}})\text{Cr}(\text{N}_2)$ product. DFT calculations suggest the N_2 binding step to be thermodynamically favorable, $\Delta G^\circ = -21.7 \text{ kcal mol}^{-1}$. N_2 bridge formation to generate **3** $\Delta G^\circ = -11.4 \text{ kcal mol}^{-1}$ was favored over $(\text{POCOP}^{\text{tBu}})\text{Cr}(\text{N}_2)$. Attempts to trap the $(\text{POCOP}^{\text{tBu}})\text{Cr}(\text{I})$ fragment by photolysis of **2** in the presence of 1 equiv PMe_3 were unsuccessful. Unexpectedly, the addition PMe_3 appears to quench the photochemical reactivity of **2** as bond homolysis was not observed; no Bn_2 or **3** was formed.

In the formation of **3** from **2**, we attempted to trap the PhCH_2^{\cdot} liberated during photolysis using TEMPO radical (TEMPO = 2,2,6,6-(tetramethylpiperidine-1-yl)oxy). However, TEMPO reacts directly with **2** generating TEMPO– Bn^{20} without exposure to blue light. Addition of 1 equiv TEMPO to **2** in benzene under N_2 formed TEMPO– Bn with unreacted **2** also present. The addition of 2 equiv of TEMPO under N_2 forms TEMPO– Bn in 77% NMR yield with the full

consumption of **2** (See ESI†). **3** is not generated in this reaction, rather, we postulate the Cr(I) fragment is trapped by TEMPO forming a Cr–TEMPO adduct,²¹ i.e. $(\text{POCOP}^{\text{tBu}})\text{Cr}(\text{I})(\text{TEMPO})$ in both reactions. Photolysis of the putative $(\text{POCOP}^{\text{tBu}})\text{Cr}(\text{I})(\text{TEMPO})$ product with 427 nm light does not generate **3**.

Time-dependent Density Functional (TD-DFT) calculations were used to evaluate the photochemical reactivity of **2** using 427 nm light. As shown in Fig. 3, the

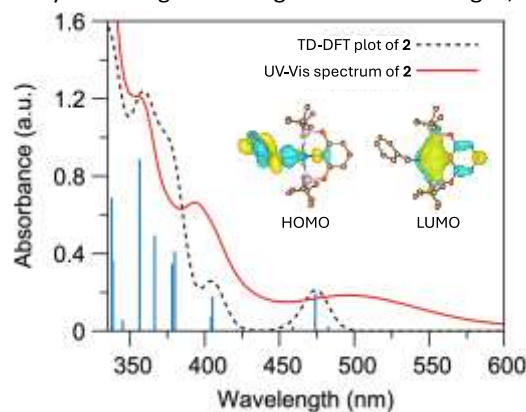


Fig. 3 Experimental UV-Vis spectrum (solid red line) of **2** recorded in toluene and the TD-DFT plot (dashed black line, scaled for comparison) of **2**. Blue bars indicate predicted electronic transitions identified by TD-DFT calculations. Frontier molecular orbitals of **2** involved in photo-induced Cr–C_{Bn} bond homolysis are shown in the inset.

calculated TD-DFT plot is in good agreement with the UV-vis spectrum of **2** (toluene) in describing the absorption band around $\lambda_{\text{max}} = 395 \text{ nm}$ ($\epsilon = 2041 \text{ M}^{-1} \text{ cm}^{-1}$). Based on the TD-DFT simulation, we assign this band as a Cr–C_{Bn} Ligand-to-Metal-Charge Transfer (LMCT). The LMCT excited state displays a significant value for the oscillator strength representing a HOMO-to-LUMO electronic transition. The spin-up (α) HOMO is characterized by a Cr–C_{Bn} σ metal-alkyl bond, whereas the LUMO level by a $d\pi$ Cr-based molecular orbital (see ESI†). An optical transition between these two levels results in homolytic bond cleavage due to its LMCT character. The feature at $\lambda_{\text{max}} = 496 \text{ nm}$ ($\epsilon = 525 \text{ M}^{-1} \text{ cm}^{-1}$) in the UV-Vis spectrum was assigned as a Cr-based d–d transition. While the TD-DFT plot does not precisely replicate the broad appearance of this band, excitation of this low-energy d–d transition does not promote Cr–C_{Bn} homolysis as **2** is unreactive to 525 nm light for 26 h.

In conclusion, this work highlights the sensitivity of the $(\text{POCOP}^{\text{tBu}})\text{Cr}(\text{II})$ fragment to the experimental conditions employed to generate a Cr– N_2 complex. While both the chemical reduction of $(\text{POCOP}^{\text{tBu}})\text{CrBr}$ and photolysis of **2** produced purple Cr products, the conventional chemical reduction route does not form the targeted Cr– N_2 complex. We describe a rare example of N_2 activation driven by visible light photolysis of a Cr-alkyl precursor (**2**) to form the dinuclear N_2 complex, **3**. Photochemically induced M–C bond homolysis may provide a general alternative strategy for the preparation of M– N_2 complexes that avoids harsh chemical reductants. Studies are underway to broaden the scope of small molecule

activation at Cr(I) by the photolysis of **2** and we are assessing the prospect of cleaving the N₂ triple bond in **3** in the development of a catalytic system for N₂ reduction to NH₃.

This material is based upon work supported by the National Science Foundation (NSF) under Grant No. CHE-1956161 and CHE-2247748. Support for MSU's NMR Center was provided by the NSF (Grant No. NSF-MRI: CHE-2018388 and DBI-1532078), the Murdock Charitable Trust Foundation (2015066:MNL), and MSU's office of the Vice President for Research and Economic Development. The authors gratefully acknowledge financial support for the X-ray diffractometer from the NSF (CHE 0619920) and an Institutional Development Award (IDeA) from the National Institute of General Medical Sciences of the National Institutes of Health (Grant # 2P20GM103432). Author contributions: O.L. Duletski, investigation, methodology, writing, editing; D. Platz, and C.J. Pollock investigation; M.A. Mosquera, computational investigation, supervision, writing; N. Arulsamy, investigation, writing; M.T. Mock, conceptualization, methodology, supervision, writing, editing, funding acquisition.

Conflicts of interest

There are no conflicts of interest to declare.

Notes and references

- (a) Y. Nishibayashi, ed., *Transition Metal–Dinitrogen Complexes: Preparation and Reactivity*, Wiley-VCH, Weinheim, 2019; (b) J. Ballmann, R. F. Munha and M. D. Fryzuk, *Chem. Commun.*, 2010, **46**, 1013-1025.
- R. J. Burford and M. D. Fryzuk, *Nat. Rev. Chem.*, 2017, **1**, 1-13.
- (a) Y. Ashida, K. Arashiba, K. Nakajima and Y. Nishibayashi, *Nature*, 2019, **568**, 536-540; (b) Y. Ashida, T. Mizushima, K. Arashiba, A. Egi, H. Tanaka, K. Yoshizawa and Y. Nishibayashi, *Nat. Synth.*, 2023, **2**, 635-644; (c) A. F. Ibrahim, P. Garrido-Barros and J. C. Peters, *ACS Catal.*, 2023, **13**, 72-78.
- (a) C. E. Laplaza and C. C. Cummins, *Science*, 1995, **268**, 861-863; (b) F. A. Darani, G. P. A. Yap and K. H. Theopold, *Organometallics*, 2023, **42**, 1324-1330; (c) Q. J. Bruch, G. P. Connor, N. D. McMillion, A. S. Goldman, F. Hasanayn, P. L. Holland and A. J. M. Miller, *ACS Catal.*, 2020, **10**, 10826-10846.
- (a) Q. J. Bruch, G. P. Connor, C. H. Chen, P. L. Holland, J. M. Mayer, F. Hasanayn and A. J. M. Miller, *J. Am. Chem. Soc.*, 2019, **141**, 20198-20208; (b) S. J. K. Forrest, B. Schlusshass, E. Y. Yuzik-Klimova and S. Schneider, *Chem. Rev.*, 2021, **121**, 6522-6587; (c) T. Miyazaki, H. Tanaka, Y. Tanabe, M. Yuki, K. Nakajima, K. Yoshizawa and Y. Nishibayashi, *Angew. Chem. Int. Ed.*, 2014, **53**, 11488-11492; (d) F. Schendzielorz, M. Finger, J. Abbesneth, C. Wurtele, V. Krewald and S. Schneider, *Angew. Chem. Int. Ed.*, 2018, **58**, 4; (e) A. J. Keane, W. S. Farrell, B. L. Yonke, P. Y. Zavalij and L. R. Sita, *Angew. Chem. Int. Ed.*, 2015, **54**, 10220-10224; (f) V. Krewald, *Dalton Trans.*, 2018, **47**, 10320-10329; (g) J. J. Curley, T. R. Cook, S. Y. Reece, P. Müller and C. C. Cummins, *J. Am. Chem. Soc.*, 2008, **130**, 9394-9405.
- (a) G. W. Margulieux, S. P. Semproni and P. J. Chirik, *Angew. Chem. Int. Ed.*, 2014, **53**, 9189-9192; (b) M. E. Fieser, J. E. Bates, J. W. Ziller, F. Furche and W. J. Evans, *J. Am. Chem. Soc.*, 2013, **135**, 3804-3807; (c) M. E. Fieser, C. W. Johnson, J. E. Bates, J. W. Ziller, F. Furche and W. J. Evans, *Organometallics*, 2015, **34**, 4387-4393.
- Y. Ashida, A. Egi, K. Arashiba, H. Tanaka, T. Mitsumoto, S. Kuriyama, K. Yoshizawa and Y. Nishibayashi, *Chem. Eur. J.*, 2022, **28**, e202200557.
- M. Fritz, S. Demeshko, C. Würtele, M. Finger and S. Schneider, *Eur. J. Inorg. Chem.*, 2023, **26**, e202300011.
- (a) C. H. Beasley, O. L. Duletski, K. S. Stankevich, N. Arulsamy and M. T. Mock, *Dalton Trans.*, 2024, **53**, 6496-6500; (b) A. J. Kendall and M. T. Mock, *Eur. J. Inorg. Chem.*, 2020, DOI: 10.1002/ejic.201901257, 1358-1375.
- (a) T. J. Hebden, R. R. Schrock, M. K. Takase and P. Müller, *Chem. Commun.*, 2012, **48**, 1851-1853; (b) J. Song, Q. Liao, X. Hong, L. Jin and N. Mezaillies, *Angew. Chem. Int. Ed.*, 2021, **60**, 12242-12247.
- D. Himmelbauer, B. Stöger, L. F. Veiros, M. Pignitter and K. Kirchner, *Organometallics*, 2019, **38**, 4669-4678.
- (a) R. Poli, *Comptes Rendus Chimie*, 2021, **24**, 147-175; (b) A. C. Brown and D. L. M. Suess, *J. Am. Chem. Soc.*, 2020, **142**, 14240-14248; (c) J. DuPont, M. B. Coxey, P. J. Schebler, C. D. Incarvito, W. G. Dougherty, G. P. A. Yap, A. L. Rheingold and C. G. Riordan, *Organometallics*, 2007, **26**, 971-979.
- (a) K. C. MacLeod, J. L. Conway, B. O. Patrick and K. M. Smith, *J. Am. Chem. Soc.*, 2010, **132**, 17325-17334; (b) Y. Champouret, U. Baisch, R. Poli, L. Tang, J. L. Conway and K. M. Smith, *Angew. Chem. Int. Ed.*, 2008, **47**, 6069-6072.
- (a) A. M. May and J. L. Dempsey, *Chem. Sci.*, 2024, **15**, 6661-6678; (b) P. M. N. Dô, N. G. Akhmedov, J. L. Petersen, B. S. Dolinar and C. Milsmann, *Chem. Commun.*, 2020, **56**, 5397-5400.
- (a) C. L. Pitman and A. J. M. Miller, *Organometallics*, 2017, **36**, 1906-1914; (b) L. J. Johnston and M. C. Baird, *J. Organomet. Chem.*, 1988, **358**, 405-409; (c) P. E. O'Connor, D. J. Berg and T. Barclay, *Organometallics*, 2002, **21**, 3947-3954; (d) H. G. Alt, *Angew. Chem. Int. Ed.*, 2003, **23**, 766-782; (e) B. E. Olafsen, G. V. Crescenzo, L. P. Moisey, B. O. Patrick and K. M. Smith, *Inorg. Chem.*, 2018, **57**, 9611-9621; (f) C. Camp, L. N. Grant, R. G. Bergman and J. Arnold, *Chem. Commun.*, 2016, **52**, 5538-5541.
- Photolysis of **2** with 370 or 390 nm LEDs also generates **3**; however, sample degradation occurs using a 370 nm LED.
- (a) J. H. Espenson, *Acc. Chem. Res.*, 1992, **25**, 222-227; (b) Cr–C_R Bond Dissociation Free Energies from DFT calculations: Cr–C_{Bn} = 32.6 kcal mol⁻¹; Cr–C_{p-Tol} = 59.0 kcal mol⁻¹. **1** is stable to the exposure of 370 nm or 390 nm light.
- S. A. Stoian, J. Vela, J. M. Smith, A. R. Sadique, P. L. Holland, E. Munck and E. L. Bominaar, *J. Am. Chem. Soc.*, 2006, **128**, 10181-10192.
- The weak coordination of N₂ at Cr in the excited-state, prior to Cr–C_{Bn} bond homolysis, cannot be ruled out in the mechanism to form **3**.
- S. Barroso, A. M. Coelho, P. Adao, M. J. Calhorda and A. M. Martins, *Dalton Trans.*, 2017, **46**, 9692-9704.
- (a) A. K. Kayser, P. T. Wolczanski, T. R. Cundari, M. M. Bollmeyer, K. M. Lancaster and S. N. MacMillan, *Chem. Commun.*, 2022, **58**, 9818-9821; (b) T. A. Nguyen, A. M. Wright, J. S. Page, G. Wu and T. W. Hayton, *Inorg. Chem.*, 2014, **53**, 11377-11387; (c) K. Kleinlein, A. J. Bendel-Smith, S. L. Zheng and T. A. Betley, *Angew. Chem. Int. Ed.*, 2017, **56**, 12197-12201.